Table 5. Comparison between diabetic and non-diabetic patients in age, baseline peritoneal transport D/P Cr, systemic factors and peritoneal pathological factors

	Diabetics	Non-diabetics	P
Number	24	18	
Age (year)	62.0 ± 13.7	64.6 ± 15.1	0.468
Men (*n*, %)	20 (83.3%)	12 (66.7%)	0.168
BMI (kg/m^2)	23.3 ± 2.7	22.4 ± 3.0	0.174
D/P Cr	0.73 ± 0.14	0.71 ± 0.13	0.639
eGFR (mL/min/1.73 m^2)	6.5 (5.1–7.7)	7.0 (5.2–8.0)	0.703
Serum albumin level (g/dL)	3.03 ± 0.74	3.66 ± 0.55	0.003
Serum CRP level (mg/dL)	0.20 (0.06–1.08)	0.18 (0.09–0.71)	0.889
CD68-positive macrophages (/mm)	13.9 (5.2–34.3)	11.3 (6.2–29.5)	0.959
IL-6-positive cells (/mm)	4.1 (1.3–7.2)	3.1 (1.4–4.4)	0.374
CD31-positive vessels (/mm)	8.5 (3.9–12.8)	7.1 (4.0–9.5)	0.360
PAL-E-positive vessels (/mm)	7.1 (4.7–12.28)	6.4 (3.5–8.6)	0.286
Chymase-positive mast cells (/mm)	5.4 (3.3–8.8)	4.0 (2.4–5.7)	0.140
Tryptase-positive mast cells (/mm)	4.7 (3.3–8.3)	4.1 (2.5–5.7)	0.227
CD3-positive cells (/mm)	3.8 (1.4–6.0)	2.9 (0.7–5.8)	0.460
MPO-positive cells (/mm)	4.9 (3.7–11.2)	5.2 (1.1–13.7)	0.723
PCV thickness (μm)	4.2 (3.5–4.6)	4.5 (3.4–5.0)	0.622

Results are expressed as means ± SD or number (percent). Variables without normal distribution are given as median (interquartile range). MPO, myeloperoxidase; PCV, post-capillary venule.

lower impact on peritoneal permeability than peritoneal local macrophage infiltration.

Mast cells are thought to participate in the inflammatory response and fibrosis through their ability to secrete various inflammatory mediators [41,42], and some mast cell mediators are known to promote angiogenesis [42]. Tryptase may contribute to vascular permeability by direct or indirect generation of bradykinin from kininogens [43]. Chymase may also play a role in tissue fibrosis through angiotensin II generation and TGF-β activation [41]. Interestingly, vasculature quantity and thickness in omentum after exposure to high-glucose PD fluid were significantly reduced in mast cell-deficient rats when compared with wild-type rats [44]. Mast cells maturing in different tissue microenvironments can vary widely in the types and amounts of tryptases and chymases expressed [45]. Therefore, we analysed both tryptase-positive mast cells and chymase-positive mast cells in normal and uraemic peritoneum. However, in the peritoneal membrane, mast cell infiltration is not likely to be an important factor in baseline peritoneal permeability, nor is the presence of T cells, B cells and neutrophils, as compared with macrophages (Figure 4).

Numerous other factors may be involved in determining the baseline peritoneal permeability of PD patients. There are many reports supporting the notion that diabetes affects peritoneal transport rate [46,47]. On the other hand, it has also been reported that high peritoneal transport status is not linked with the presence of diabetes [8,48,49]. In our analysis, we found that diabetic patients had significantly lower serum albumin levels than non-diabetic patients; however, there were no differences in peritoneal permeability, density of inflammatory cells and blood vessels and CRP levels between the two groups (Table 5). Taken together, these data suggest that diabetes is not the major determinant of baseline peritoneal transport.

In conclusion, we showed that local macrophage infiltration is associated with uraemia and baseline high peritoneal solute transport. Further *in vivo* and *in vitro* studies are required in order to clarify the role of local macrophage infiltration in baseline peritoneal membrane conditions for PD.

Supplementary data

Supplementary data is available online at http://ndt.oxfordjournals.org.

Acknowledgements. The authors would like to express their gratitude to Dr Takeshi Wakai (Department of Preventive Medicine/Biostatistics and Medical Decision Making, Nagoya University, Nagoya, Japan) for discussion of statistical analysis. The technical assistance of Mr Norihiko Suzuki, Ms Keiko Higashide, Ms Naoko Asano and Ms Yuriko Sawa (Department of Nephrology, Nagoya University) is also gratefully acknowledged.

Conflict of interest statement. None declared.

References

1. Churchill DN, Thorpe KE, Nolph KD *et al.* Increased peritoneal membrane transport is associated with decreased patient and technique survival for continuous peritoneal dialysis patients. The Canada-USA (CANUSA) Peritoneal Dialysis Study Group. *J Am Soc Nephrol* 1998; 9: 1285–1292
2. Rumpsfeld M, McDonald SP, Johnson DW. Higher peritoneal transport status is associated with higher mortality and technique failure in the Australian and New Zealand peritoneal dialysis patient populations. *J Am Soc Nephrol* 2006; 17: 271–278
3. Kawaguchi Y, Ishizaki T, Imada A *et al.* Searching for the reasons for drop-out from peritoneal dialysis: a nationwide survey in Japan. *Perit Dial Int* 2003; 23: S175–S177
4. Brimble KS, Walker M, Margetts PJ *et al.* Meta-analysis: peritoneal membrane transport, mortality, and technique failure in peritoneal dialysis. *J Am Soc Nephrol* 2006; 17: 2591–2598
5. Flessner M. The transport barrier in intraperitoneal therapy. *Am J Physiol Renal Physiol* 2005; 288: F433–F442
6. Mizuno M, Ito Y, Hepburn N *et al.* Zymosan, but not lipopolysaccharide, triggers severe and progressive peritoneal injury accompan-

ied by complement activation in a rat peritonitis model. *J Immunol* 2009; 183: 1403–1412
7. Chung SH, Chu WS, Lee HA *et al.* Peritoneal transport characteristics, comorbid diseases and survival in CAPD patients. *Perit Dial Int* 2000; 20: 541–547
8. Rumpsfeld M, McDonald SP, Purdie DM *et al.* Predictors of baseline peritoneal transport status in Australian and New Zealand peritoneal dialysis patients. *Am J Kidney Dis* 2004; 43: 492–501
9. Menon V, Greene T, Wang X *et al.* C-reactive protein and albumin as predictors of all-cause and cardiovascular mortality in chronic kidney disease. *Kidney Int* 2005; 68: 766–772
10. Wang AY, Woo J, Lam CW *et al.* Is a single time point C-reactive protein predictive of outcome in peritoneal dialysis patients? *J Am Soc Nephrol* 2003; 14: 1871–1879
11. Margetts PJ, McMullin JP, Rabbat CG *et al.* Peritoneal membrane transport and hypoalbuminemia: cause or effect? *Perit Dial Int* 2000; 20: 14–18
12. Pecoits-Filho R, Carvalho MJ, Stenvinkel P *et al.* Systemic and intraperitoneal interleukin-6 system during the first year of peritoneal dialysis. *Perit Dial Int* 2006; 26: 53–63
13. Oh KH, Moon JY, Oh J *et al.* Baseline peritoneal solute transport rate is not associated with markers of systemic inflammation or comorbidity in incident Korean peritoneal dialysis patients. *Nephrol Dial Transplant* 2008; 23: 2356–2364
14. Rodrigues AS, Almeida M, Fonseca I *et al.* Peritoneal fast transport in incident peritoneal dialysis patients is not consistently associated with systemic inflammation. *Nephrol Dial Transplant* 2006; 21: 763–769
15. Pecoits-Filho R, Araújo MR, Lindholm B *et al.* Plasma and dialysate IL-6 and VEGF concentrations are associated with high peritoneal solute transport rate. *Nephrol Dial Transplant* 2002; 17: 1480–1486
16. Kihm LP, Wibisono D, Müller-Krebs S *et al.* RAGE expression in the human peritoneal membrane. *Nephrol Dial Transplant* 2008; 23: 3302–3306
17. de Waal RM, van Altena MC, Erhard H *et al.* Lack of lymphangiogenesis in human primary cutaneous melanoma. Consequences for the mechanism of lymphatic dissemination. *Am J Pathol* 1997; 150: 1951–1957
18. Matsuo S, Imai E, Horio M *et al.* Revised equations for estimated GFR from serum creatinine in Japan. *Am J Kidney Dis* 2009; 53: 982–992
19. Twardowski ZJ. The fast peritoneal equilibration test. *Semin Dial* 1990; 3: 141–142
20. Honda K, Hamada C, Nakayama M *et al.* Peritoneal Biopsy Study Group of the Japanese Society for Peritoneal Dialysis. Impact of uremia, diabetes, and peritoneal dialysis itself on the pathogenesis of peritoneal sclerosis: a quantitative study of peritoneal membrane morphology. *Clin J Am Soc Nephrol* 2008; 3: 720–728
21. Mizutani M, Ito Y, Mizuno M *et al.* Connective tissue growth factor (CTGF/CCN2) is increased in peritoneal dialysis patients with high peritoneal solute transport rate. *Am J Physiol Renal Physiol* 2009; 298: F721–F733
22. Nishimura H, Ito Y, Mizuno M *et al.* Mineralocorticoid receptor blockade ameliorates peritoneal fibrosis in new rat peritonitis model. *Am J Physiol Renal Physiol* 2008; 294: F1084–F1093
23. Sakamoto I, Ito Y, Mizuno M *et al.* Lymphatic vessels develop during tubulointerstitial fibrosis. *Kidney Int* 2009; 75: 828–838
24. Del Peso G, Jiménez-Heffernan JA, Bajo MA *et al.* Epithelial-to-mesenchymal transition of mesothelial cells is an early event during peritoneal dialysis and is associated with high peritoneal transport. *Kidney Int Suppl* 2008; 108: S26–S33
25. Alscher DM, Braun N, Biegger D *et al.* Peritoneal mast cells in peritoneal dialysis patients, particularly in encapsulating peritoneal sclerosis patients. *Am J Kidney Dis* 2007; 49: 452–461
26. Williams JD, Craig KJ, Topley N *et al.* Morphologic changes in the peritoneal membrane of patients with renal disease. *J Am Soc Nephrol* 2002; 13: 470–479
27. Gillerot G, Goffin E, Michel C *et al.* Genetic and clinical factors influence the baseline permeability of the peritoneal membrane. *Kidney Int* 2005; 67: 2477–2487
28. Zweers MM, Struijk DG, Smit W *et al.* Vascular endothelial growth factor in peritoneal dialysis: a longitudinal follow-up. *J Lab Clin Med* 2001; 137: 125–132
29. Berse B, Brown LF, Van de Water L *et al.* Vascular permeability factor (vascular endothelial growth factor) gene is expressed differentially in normal tissues, macrophages, and tumors. *Mol Biol Cell* 1992; 3: 211–220
30. Pérez-Ruiz M, Ros J, Morales-Ruiz M *et al.* Vascular endothelial growth factor production in peritoneal macrophages of cirrhotic patients: regulation by cytokines and bacterial lipopolysaccharide. *Hepatology* 1999; 29: 1057–1063
31. Ali MH, Schlidt SA, Chandel NS *et al.* Endothelial permeability and IL-6 production during hypoxia: role of ROS in signal transduction. *Am J Physiol* 1999; 277: L1057–L1065
32. McLaren J, Prentice A, Charnock-Jones DS *et al.* Vascular endothelial growth factor is produced by peritoneal fluid macrophages in endometriosis and is regulated by ovarian steroids. *J Clin Invest* 1996; 15: 482–489
33. Topley N, Jörres A, Luttmann W *et al.* Human peritoneal mesothelial cells synthesize interleukin-6: induction by IL-1 beta and TNF alpha. *Kidney Int* 1993; 43: 226–233
34. Mandl-Weber S, Cohen CD, Haslinger B *et al.* Vascular endothelial growth factor production and regulation in human peritoneal mesothelial cells. *Kidney Int* 2002; 61: 570–578
35. Wang T, Heimbürger O, Cheng HH *et al.* Does a high peritoneal transport rate reflect a state of chronic inflammation? *Perit Dial Int* 1999; 19: 17–22
36. Chung SH, Heimbürger O, Stenvinkel P *et al.* Association between inflammation and changes in residual renal function and peritoneal transport rate during the first year of dialysis. *Nephrol Dial Transplant* 2001; 16: 2240–2245
37. Honda H, Qureshi AR, Heimbürger O *et al.* Serum albumin, C-reactive protein, interleukin 6, and fetuin a as predictors of malnutrition, cardiovascular disease, and mortality in patients with ESRD. *Am J Kidney Dis* 2006; 47: 139–148
38. Iseki K, Tozawa M, Yoshi S *et al.* Serum C-reactive protein (CRP) and risk of death in chronic dialysis patients. *Nephrol Dial Transplant* 1999; 14: 1956–1960
39. Stenvinkel P, Lindholm B. C-reactive protein in end-stage renal disease: are there reasons to measure it? *Blood Purif* 2005; 23: 72–78
40. Stenvinkel P, Wanner C, Metzger T *et al.* Inflammation and outcome in end-stage renal failure: does female gender constitute a survival advantage? *Kidney Int* 2002; 62: 1791–1798
41. Holdsworth SR, Summers SA. Role of mast cells in progressive renal diseases. *J Am Soc Nephrol* 2008; 19: 2254–2261
42. Nigrovic PA, Lee DM. Mast cells in inflammatory arthritis. *Arthritis Res Ther* 2005; 7: 1–11
43. Miller HR, Pemberton AD. Tissue-specific expression of mast cell granule serine proteinases and their role in inflammation in the lung and gut. *Immunology* 2002; 105: 375–390
44. Zareie M, Fabbrini P, Hekking LH *et al.* Novel role for mast cells in omental tissue remodeling and cell recruitment in experimental peritoneal dialysis. *J Am Soc Nephrol* 2006; 17: 3447–3457
45. Metcalfe DD, Baram D, Mekori YA. Mast cells. *Physiol Rev* 1997; 77: 1033–1079
46. Lamb EJ, Worrall J, Buhler R *et al.* Effect of diabetes and peritonitis on the peritoneal equilibration test. *Kidney Int* 1995; 47: 1760–1767
47. Nakamoto H, Imai H, Kawanishi H *et al.* Effect of diabetes on peritoneal function assessed by personal dialysis capacity test in patients undergoing CAPD. *Am J Kidney Dis* 2002; 40: 1045–1054
48. Smit W, van Esch S, Struijk DG *et al.* Free water transport in patients starting with peritoneal dialysis: a comparison between diabetic and non diabetic patients. *Adv Perit Dial* 2004; 20: 13–17
49. Chou MY, Kao MT, Lai MN *et al.* Comparisons of the peritoneal equilibration test and ultrafiltration in patients with and without diabetes mellitus on continuous ambulatory peritoneal dialysis. *Am J Nephrol* 2006; 26: 87–90

Received for publication: 11.02.10; Accepted in revised form: 25.10.10

Cell Metabolism, *Volume 12*

Supplemental Information

A Liver-Derived Secretory Protein, Selenoprotein P, Causes Insulin Resistance

Hirofumi Misu, Toshinari Takamura, Hiroaki Takayama, Hiroto Hayashi, Naoto Matsuzawa-Nagata, Seiichiro Kurita, Kazuhide Ishikura, Hitoshi Ando, Yumie Takeshita, Tsuguhito Ota, Masaru Sakurai, Tatsuya Yamashita, Eishiro Mizukoshi, Taro Yamashita, Masao Honda, Ken-ichi Miyamoto, Tetsuya Kubota, Naoto Kubota, Takashi Kadowaki, Han-Jong Kim, In-kyu Lee, Yasuhiko Minokoshi, Yoshiro Saito, Kazuhiko Takahashi, Yoshihiro Yamada, Nobuyuki Takakura, and Shuichi Kaneko

Supplemental Experimental Procedures

Human clinical studies

Liver samples to be analyzed by SAGE were obtained from five patients with type 2 diabetes and five non-diabetic subjects who underwent surgical procedures for malignant tumors, including gastric cancer, gall bladder cancer, and colon cancer. Liver samples to be subjected to DNA chip analysis were obtained from 22 patients with type 2 diabetes and 11 subjects with normal glucose tolerance using ultrasonography-guided biopsy needles. Detailed clinical information about these subjects is presented elsewhere(Misu et al., 2007). Serum samples were obtained from 35 patients with type 2 diabetes and eight subjects with normal glucose tolerance. Following an overnight fast, a venous blood samples were taken from each patient. The HOMA-IR was calculated using the following formula: HOMA-IR = [fasting insulin (μU/ml) x fasting plasma glucose (mmol/L)] / 22.5(Matthews et al., 1985). All patients provided written informed consent for participation in this study. All experimental protocols were approved by the relevant ethics committees in our institution and were conducted in accordance with the Declaration of Helsinki.

SAGE and DNA chip analyses

Extraction of RNA from human liver tissue, SAGE, Affymetrix gene chip hybridization, and DNA chip analysis were performed as previously described(Misu et al., 2007).

Measurement of serum SeP levels in human subjects

Serum levels of SeP were measured (using two monoclonal antibodies) by ELISA, as described previously(Saito et al., 2001).

Glucose clamping in humans subjects

Insulin sensitivity in patients with type 2 diabetes was evaluated using the glucose clamp method(DeFronzo et al., 1979). The euglycemic–hyperinsulinemic clamp technique was performed using an artificial pancreas (model STG-22; Nikkiso, Tokyo, Japan), as previously described(Nagai et al., 1999). Insulin was infused at a rate of 3.0 mU/kg per minute, resulting in a steady-state insulin concentration of approximately 250-350 μU/ml(Sakurai et al., 2007). Insulin sensitivity was measured in terms of the glucose metabolic clearance rate (MCR) of glucose in mg/kg/min.

Materials

H4IIEC, 3T3-L1, and C2C12 cells were purchased from the American Type Culture Collection (ATCC, Manassas, VA). Human recombinant insulin was purchased from Sigma–Aldrich (St. Louis, MO). Rabbit anti-phospho-Akt (Ser473) monoclonal antibody, rabbit anti-total Akt polyclonal antibody, rabbit anti-PTEN (phosphatase and tensin homologue deleted on chromosome 10) polyclonal antibody, rabbit anti-insulin receptor β monoclonal antibody, mouse anti-phosphotyrosine monoclonal antibody (P-Tyr-100), rabbit anti-LKB1 monoclonal antibody, rabbit anti-phospho-AMPK (Thr172) monoclonal antibody, and rabbit anti-phospho-ACC (Ser79) polyclonal antibody were purchased from Cell Signaling (Danvers, MA). Rabbit anti-selenoprotein P polyclonal antibody (sc-30162) and rabbit anti-GAPDH polyclonal antibody

were obtained from Santa Cruz Biotechnology (Santa Cruz, CA). Rabbit anti-insulin receptor substrate-2 polyclonal antibody was purchased from Upstate Biotechnology (Charlottesville, VA).

Measurement of serum SeP levels in mice

Serum or plasma was diluted 50 times in a standard detergent-containing buffer. Proteins were separated by 5–20% sodium dodecyl sulphate polyacrylamide gel electrophoresis (SDS-PAGE) and transferred to polyvinylidene difluoride membrane (PVDM). Membranes were probed with a rabbit anti-selenoprotein P polyclonal antibody. Densitometric analysis of blotted membranes was performed using ImageJ software, available from the NIH website (http://rsb.info.nih.gov/ij/).

Measurement of hepatocyte glucose release and expression of mRNAs encoding gluconeogenic enzymes

H4IIEC cells were grown in six-well plates to 70–80% confluence in Dulbecco's Modified Eagle Medium (DMEM) supplemented with 20% horse serum and 5% fetal bovine serum. Cells were washed twice with phosphate-buffered saline (PBS) and stimulated through treatment with gluconeogenesis buffer (glucose-free DMEM containing 3.7 g/L sodium bicarbonate, 5 mM sodium pyruvate, 50 mM sodium lactate, 1 mM cAMP, and 250 nM dexamethasone). 1 ng/ml of human insulin was used to suppress glucose release. After a 24-h incubation period, we measured the release of glucose into the culture medium using a glucose oxidation kit (Sigma–Aldrich). Total RNA was isolated from treated cells. Levels of mRNAs encoding gluconeogenic enzymes were measured by real-time PCR.

Measurement of glucose uptake into mouse C2C12 myoblasts

C2C12 skeletal muscle myoblasts were maintained in DMEM supplemented with 10% fetal bovine serum. To induce myogenic differentiation, the cells were subsequently maintained in DMEM containing 0.5% horse serum for 7 days. Basal and insulin-stimulated glucose transportation were estimated by measuring 2-deoxy-[^{3}H]glucose uptake. Briefly, differentiated cells were pretreated with purified SeP or vehicle for 12 h. They were then washed twice in PBS. Following incubation in glucose-free DMEM (Invitrogen) in the presence or absence of 1000 ng/ml insulin for 60 min at 37°C, 2-deoxy-glucose (final concentration: 100 μM) and 2-deoxy-[^{3}H]glucose (final concentration: 0.25 μCi/ml; Amersham) were added to the culture medium. Glucose uptake was stopped after 10 min by washing the cells three times in cold PBS containing 0.1 mM phloretin (Sigma–Aldrich), which is known to block glucose transporters. Data were corrected for non-transporter-mediated uptake, and cell surface binding was measured in the presence of 1 mM phloretin.

Measurement of fatty acid oxidation in H4IIEC hepatocytes

H4IIEC hepatocytes were treated with purified human SeP for 3 h and then washed with DMEM prior to labeling in DMEM containing 0.4 mM oleate, 1.5% bovine serum albumin, and [^{14}C]oleate (1 μCi/ml) (NEC317; PerkinElmer Life Sciences) for 1 h. Assessment of fatty acid oxidation products was performed as described previously(Reid et al., 2008), with modifications. Briefly, the labeling medium was collected and centrifuged, and the supernatant was transferred to a 25-ml flask with a center well (Kontes) containing filter paper saturated with 100 μl of 1M KOH. After the flask was sealed with a stopper, 200 μl of 70% perchloric acid was added to the labeling medium to release [^{14}C]CO_2. The flask was then rocked at 37°C for 1 h. The saturated filter paper containing trapped [^{14}C]CO_2 was assessed for radioactivity in a liquid scintillation counter.

RNA isolation, cDNA synthesis, and real-time PCR analysis

Total RNA was isolated from cells using the QuickGene system (FujiFilm, Tokyo, Japan). cDNA was synthesized from 100 ng of total RNA using a high-capacity cDNA Archive Kit (Applied Biosystems, Foster City, CA). Real-time PCR analysis was performed as previously described(Misu et al., 2007). Primer sets and TaqMan probes were proprietary to Applied Biosystems (Assays-on-Demand Gene Expression Products). To control for variation in the amount of DNA available for PCR, target gene expression in each sample was normalized relative to the expression of an endogenous control (β-actin RNA or 18s rRNA) (TaqMan Control Reagent Kit; Applied Biosystems).

Western blot studies in hepatocytes

H4IIEC hepatocytes or mouse primary hepatocytes were grown in 24-well multi-plates. Cells were serum-starved and incubated in DMEM supplemented with the indicated reagents for 24 h. Following treatment with SeP or BSO for 24 h, cells were stimulated with 1 ng/ml human recombinant insulin for 15 min. They were then washed in ice-cold PBS and lysed at 4°C in a buffer containing 20 mmol/L Tris, 5 mmol/L EDTA, 10 mmol/L $Na_4P_2O_7$, 1% NP-40, 1% protease inhibitor cocktail (Sigma–Aldrich), and 1% phosphatase inhibitor cocktail (Pierce, Rockford, IL). Lysates were then centrifuged to remove insoluble

material. Samples were sonicated with BIORUPTOR® (Cosmo Bio, Tokyo, Japan). Whole-cell lysates were then separated by 5–20% SDS-PAGE and transferred to PVDM, using Bio-Rad Trans-Blot apparatus. Membranes were blocked in a buffer containing 50 mM Tris, 150 mM NaCl, 0.1% Tween 20, and 5% nonfat milk (pH 7.5) for 1 h at 20°C. They were then probed with antibodies for 2 h at 20°C or for 16 h at 4°C. Afterward, membranes were washed in a buffer containing 50 mM Tris, 150 mM NaCl, and 0.1% Tween 20, pH 7.5 and then incubated with horseradish peroxidase-linked secondary antibody. Protein signals were detected using ECL plus reagent, according to the manufacturer's instructions (Amersham Biosciences Corp., Piscataway, NJ). Densitometric analysis of blotted membranes was performed using ImageJ software.

Injection of purified SeP into mice

Prior to glucose and insulin tolerance testing or Western blot analysis, 10-week-old female C57BL/6J mice were twice injected intraperitoneally with purified human SeP (1 mg/kg body weight). Control mice were injected with an identical volume of PBS (vehicle). Injections were administered 12 and 2 h before tolerance testing. Two hours after the second injection, glucose and insulin tolerance tests or Western blot analysis was performed.

Glucose and insulin tolerance tests in mice

In preparation for glucose tolerance testing, mice were fasted for 12 h. After fasting, glucose was administered intraperitoneally, and blood glucose levels were measured at 0–120 min. For insulin tolerance testing, mice were fasted for 4 h. After fasting, insulin was administered intraperitoneally, and blood glucose levels were measured.

Western blot studies in mice

Ten-week-old female C57BL 6/J mice were injected intraperitoneally with purified human SeP 12 and 2 h before insulin stimulation. Control mice were injected with PBS (vehicle). Two hours after the second injection of purified SeP or vehicle, mice were injected intraperitoneally with human insulin (10 units/kg body weight). Twenty minutes later, mice were anesthetized and sacrificed to allow isolation of liver and hindlimb muscle tissue. Tissue samples were homogenized using a Polytron homogenizer running at half-maximal speed (15,000 rpm) for 1 min on ice in 1000 μl of homogenization buffer containing 20 mmol/L Tris, 5 mmol/L EDTA, 10 mmol/L $Na_4P_2O_7$, 1% NP-40, 1% protease inhibitor cocktail (Sigma–Aldrich), and 1% phosphatase inhibitor cocktail (Pierce). Tissue lysates were solubilized by continuous stirring for 1 h at 4°C and centrifuged for 60 min at 14 000 × *g*. Protein samples were separated by 5–20% SDS-PAGE and transferred to PVDM. Serine phosphorylation of specific target proteins was analyzed by Western blotting.

Hyperinsulinemic–euglycemic clamp studies in mice

Clamp studies were performed as described previously(Kubota et al., 2006), with slight modifications. Briefly, 2–3 days before the study, an infusion catheter was inserted into the right jugular vein of test animals under general anesthesia induced using sodium pentobarbital. Prior to the clamp study, 10-week-old female C57BL/6J mice were injected intraperitoneally twice with purified human SeP (1 mg/kg body weight) or PBS. Injections were administered 12 and 2 h before the clamp study. Clamp studies were performed on conscious and unrestrained animals. Insulin (Novolin R; Novo Nordisk, Denmark) was continuously infused at a rate of 5.0 mU/kg/min, and the blood glucose concentration (monitored every 5 min) was maintained at 100 mg/dl through the administration of glucose (50%, enriched to approximately 20% with [6,6-$^2H_2$]glucose; Sigma) for 120 min. Blood was sampled through tail-tip bleeds at 90, 105, and 120 min for the purpose of determining the rate of glucose disappearance (Rd). Rd values were calculated according to non-steady-state equations, and hepatic glucose production (HGP) was calculated as the difference between the Rd and the exogenous glucose infusion rates (GIR)(Kubota et al., 2006).

Blood samples assays in mice

Serum levels of insulin, glucagon, GLP-1, and GIP were determined using a mouse insulin ELISA kit (Morinaga), a YK090 glucagon EIA kit (Yanaihara), a YK160 GLP-1 EIA kit (Yanaihara), and a mouse GIP ELISA kit (Millipore), respectively, according to the manufacturers' instructions. To allow measurement of active GIP and active GLP-1 levels, DPPIV inhibitor (Millipore) was added to the blood samples during their collection. Active GLP-1 was determined using active GLP-1 ELISA kit (Millipore). Serum NEFA levels were assayed by enzymatic methods (Wako Pure Chemical Industries Ltd., Osaka, Japan).

siRNA transfection in H4IIEC hepatocytes
H4IIEC hepatocytes were transiently transfected with 30 nM of siRNA duplex oligonucleotides using Lipofectamine RNAiMAX (Invitrogen) according to the manufacturer's instructions. A *Sepp1*-specific siRNA with the following sequence was synthesized by B-Bridge International, Inc. (Tokyo, Japan): 5'-CAGUAAGCCUUCAGAGAAUTT-3' (sense). Negative control siRNA was purchased from B-Bridge. Two days after transfection, cells were stimulated with 1 ng/ml of human recombinant insulin for 15 min.

Measurement of AMP and ATP content
Liver or H4IIEC hepatocytes were homogenized in 10% perchloric acid. The resulting lysates were then neutralized through the addition of NaOH. Supernatant AMP and ATP content was measured by high-performance liquid chromatography (HPLC)(Watanabe et al., 1989).

Adenovirus-mediated gene transfer in H4IIEC hepatocytes
H4IIEC hepatocytes were grown to 90% confluence in 24-well multi-plates. Cells were infected with adenoviruses encoding dominant negative α1 and α2 AMPK or LacZ for 4 h (8.9 X 106 PFU/well) (Minokoshi et al., 2004). We expressed α1 and α2 dominant negative AMPK simultaneously to maximize the effect on AMPK activity. After removing the adenoviruses, the cells were incubated with DMEM for 24 h. Then, following treatment with purified SeP protein or vehicle for 24 h, they were stimulated with 1 ng/ml of human recombinant insulin for 15 min. They were then washed in ice-cold PBS and lysed at 4°C in a buffer containing 20 mmol/L Tris, 5 mmol/L EDTA, 10 mmol/L $Na_4P_2O_7$, 1% NP-40, 1% protease inhibitor cocktail (Sigma–Aldrich), and 1% phosphatase inhibitor cocktail (Pierce, Rockford, IL).

Indirect calorimetry
Mice were housed in standard metabolic cages for 24 h. An indirect calorimetry system was used, in conjunction with the computer-assisted data acquisition program Chart5.2 (AD Instruments, Sydney, Australia), to measure and record oxygen consumption and carbon dioxide production at 5-minute intervals.

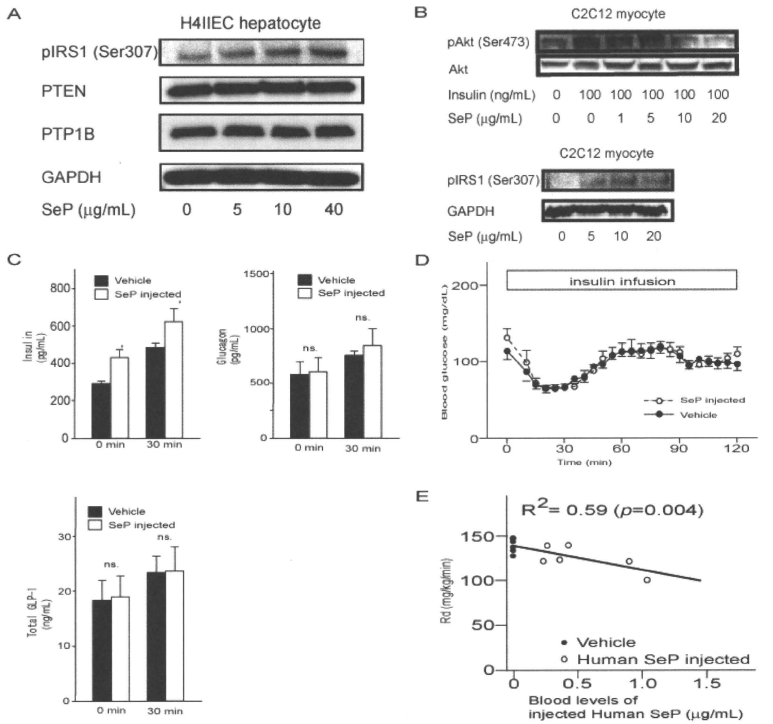

Figure S1. SeP Impairs Insulin Signaling *In Vitro* and *In Vivo*, Related to Figure 3
(**A**) Levels of pIRS1 (phosphorylate at Ser307), PTEN, and PTP1B in SeP-treated H4IIEC hepatocytes. H4IIEC hepatocytes were treated with human SeP for 12 h. Protein levels were detected by Western blotting.
(**B**) Effects of SeP on insulin-stimulated Akt phosphorylation and levels of pIRS1 (phosphorylated at Ser307) in C2C12 myocytes. To induce differentiation, C2C12 mouse skeletal myoblasts were cultured in DMEM supplemented with 0.5% horse serum for 72 h. After differentiation, cells were treated with human SeP for 72 h. After treatment with SeP, cells were stimulated with insulin for 15 min.
(**C**) Blood levels of insulin, glucagon, and GLP-1 during glucose tolerance test in mice injected with SeP or vehicle ($n = 5$). $*p < 0.05$ versus vehicle-treated mice. All data represent the mean ± SEM.
(**D**) Time course of blood glucose levels during hyperinsulinemic–euglycemic glucose clamp in mice injected with SeP or vehicle ($n = 6$).
(**E**) Negative correlation between blood levels of SeP and glucose disposal rate (Rd) in C57BL6/J mice injected with human SeP. Blood levels of injected human SeP were determined by ELISA.

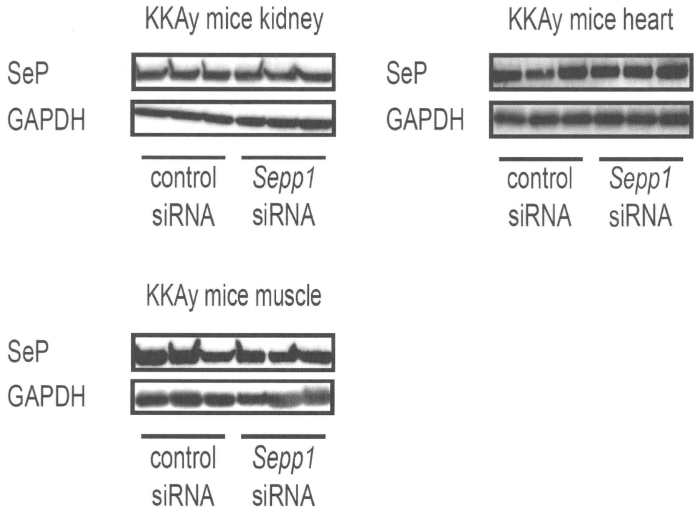

Figure S2. SeP Production in the Kidney, Heart, and Muscle of KKAy Mice Injected with Control or *Sepp1*-Specific siRNA, Related to Figure 4

SeP protein levels were measured by Western blotting 4 days after injection of siRNA. SeP levels in these tissues except the liver were unchanged by hydrodynamic injection with *Sepp1* siRNA.

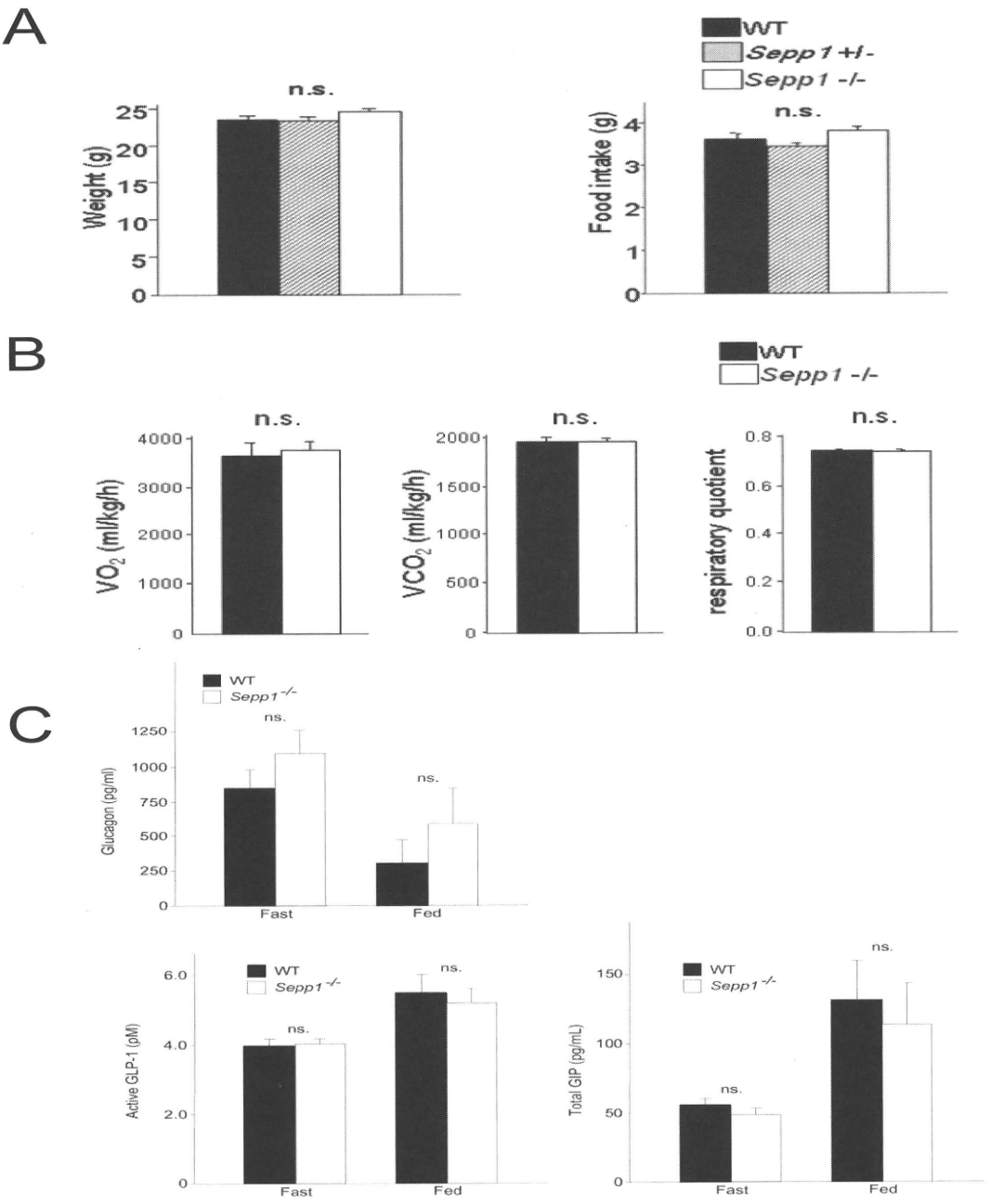

Figure S3. Parameters of *Sepp1*-Deficient Mice Fed a Regular Diet, Related to Figure 5

(**A**) Body weight and food intake in *Sepp1*-deficient mice. Data represent the mean ± SEM.

(**B**) VO_2 consumption, VCO_2 consumption, and respiratory quotients in *Sepp1*-deficient mice. Each parameter was measured by indirect calorimetry during a 24-h period. Test animals had free access to food and water. Data represent the mean ± SEM.

(**C**) Blood levels of glucagon, active GLP-1, and total GIP in fasted and fed *Sepp1*$^{-/-}$ mice (n = 6–7). DPPIV inhibitor was added to the blood samples during their collection. Active GLP-1 was determined using active GLP-1 ELISA kit. GIP was determined by an ELISA kit for total GIP. When we did not add DPPIV inhibitor, we could detect no GIP by using this kit, suggesting that a major part of GIP we measured is DPPIV-sensitive and active. Data represent the mean ± SEM.

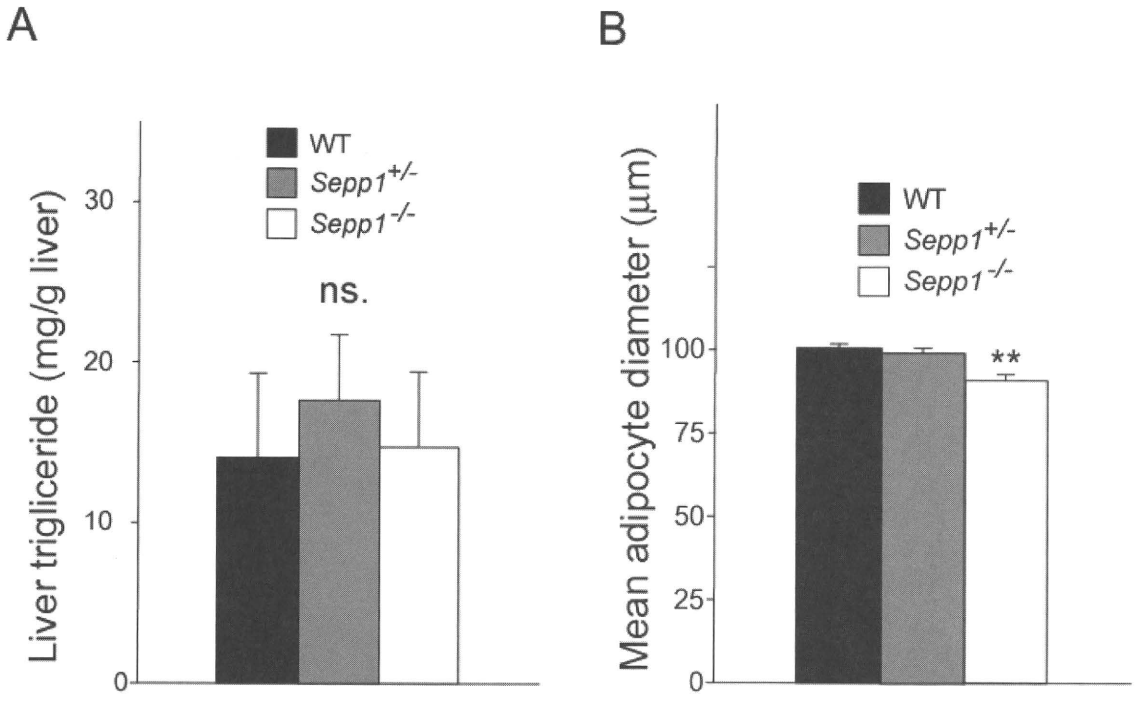

Figure S4. Parameters of *Sepp1*-Deficient Mice Fed a High Sucrose, High Fat Diet, Related to Figure 6

(**A**) Liver triglyceride content in *Sepp1*-deficient and wild-type mice fed HFHSD (n = 4–7)

(**B**) Mean Adipocyte diameter of epididymal fat in *Sepp1*-deficient and wild-type mice fed a high-fat, high-sucrose diet. Data represent the mean ± SEM. $^{**}p < 0.01$ (versus wild-type mice). We determined mean adipocyte diameter by measuring at least 300 adipocytes randomly selected from four independent sections.

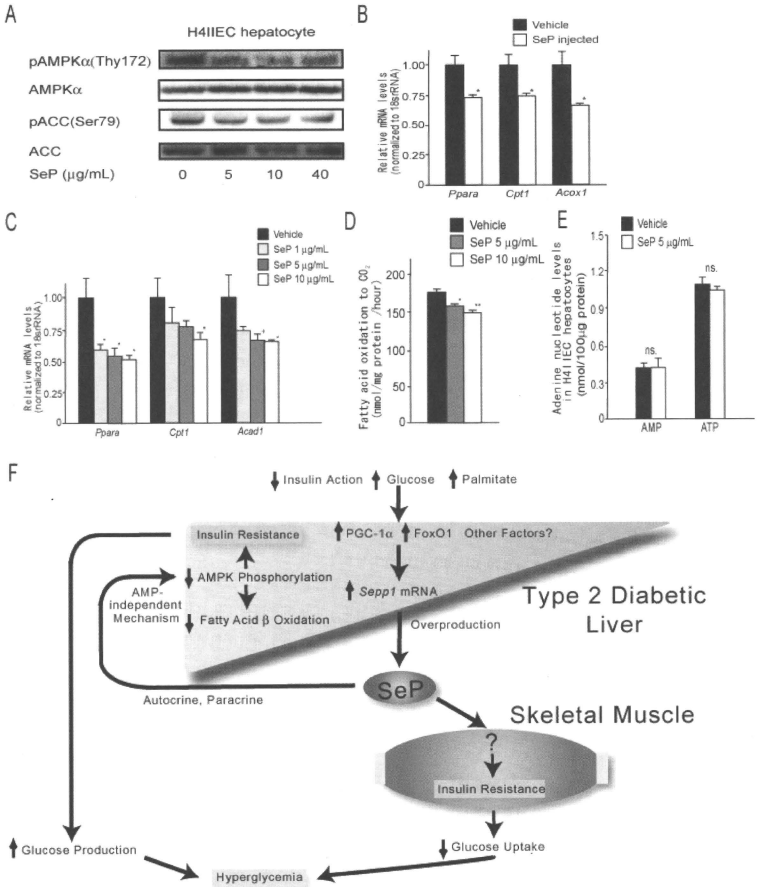

Figure S5. SeP Reduces Phosphorylation of AMPK, Related to Figure 7
(**A**) Levels of pAMPK (phosphorylated at Thr172) and pACC (Ser79) in SeP-treated H4IIEC hepatocytes. H4IIEC hepatocytes were treated with human SeP for 12 h.
(**B**) Expression of genes involved in β-oxidation in the liver in C57BL6/J mice injected with SeP or vehicle. Purified SeP protein (1 mg/kg body weight) was injected via the tail vein. Six hours later, animals were anesthetized and killed and liver tissue isolated. Data represent the mean ± SEM. $*p < 0.05$ (versus vehicle-treated mice).
(**C**) Expression of genes involved in β-oxidation in H4IIEC hepatocytes treated with SeP. Cells ($n = 5$) were treated with purified human SeP at the indicated concentrations for 24 h. Data represent the mean ± SEM. $*p < 0.05$; $^{+}p = 0.08$ (versus vehicle-treated cells).
(**D**) Effects of SeP on β-oxidation in H4IIEC hepatocytes. Cells ($n = 5$) were pretreated with purified human SeP at the indicated concentrations for 3 h, and then incubated for 1 h

with [^{14}C]oleate and 1.5% bovine serum albumin. Oleate oxidation was determined by measuring the release of [^{14}C]CO_2 into the culture medium. Data represent the mean ± SEM. *$p < 0.05$, **$p < 0.01$ (versus vehicle-treated cells).
(**E**) Levels of adenine nucleotides in H4IIEC hepatocytes treated with SeP or vehicle. H4IIEC hepatocytes ($n = 6$) were treated with SeP for 12 h. Data represent the mean ± SEM.
(**F**) Hepatic overproduction of SeP causes insulin resistance in obese individuals and type 2 diabetic patients. Decreased insulin action and excessive glucose or fatty acid uptake up-regulates *Sepp1* mRNA in the liver of obese subjects and type 2 diabetes patients, leading to the elevation of circulating SeP levels. SeP reduces hepatic AMPK phosphorylation and induces hepatic insulin resistance in an autocrine/paracrine manner. Insulin resistance in the skeletal muscle is further induced through an AMPK-independent mechanism. SeP-mediated insulin resistance in these two tissues contributes to hyperglycemia.

Table S1. Clinical Characteristics of the Human Subjects Whose Liver Tissue Was Subjected to DNA Chip Analysis, Related to Figure 1

	NGT	DM
n	7	10
Age (years)	45.0±14.8	50.6±12.0
Sex (M/F)	4/4	6/4
Body mass index (kg/m^2)	25.9±5.1	30.0±5.1
Fasting plasma glucose (mg/dl)	91.1±7.0	128.6±40.5*
HbA1c (%)	5.0±0.6	6.8±1.4**
HOMA-IR	2.21±1.05	3.60±3.0
Metabolic clearance rate (mg/kg/min)	7.72±2.24	5.49±3.80
Total cholesterol (mg/dl)	187.2±35.0	218.4±62.7
Triglyceride (mg/dl)	175.7±117.5	151.5±98.3
Gene expression levels of SEPP1 in liver	0.68±0.26	1.01±0.35*

Data are mean ± SD

** p <0.01 vs NGT

* p <0.05 vs NGT

NGT, normal glucose tolerance; HbA_{1c}, hemoglobin A_{1c}; HOMA-IR, homeostasis model assessment for insulin resistance. Liver biopsies were obtained following overnight fasting. Patients with type 2 diabetes were treated by diet therapy alone or using insulin. None of the subjects was receiving an oral hypoglycemic agent.

Table S2. Candidate Hepatokine Genes Involved in Insulin Resistance, Related to Figure 1

Unigene	Symbol	Name	DM/NGT ,by SAGE	p value vs.MCR	correlation coefficient
Hs.97220	CHAD	chondroadherin	45.17	0.022	0.649
Hs.275775	SEPP1	selenoprotein P, plasma, 1n	8.33	0.021	-0.656
Hs.75445	SPARCL1	SPARC-like 1 (mast9, hevin)	6.82	0.034	-0.613
Hs.435782	F13B	coagulation factor XIII, B polypeptide	3.41	0.043	-0.59
Hs.181301	CTSS	cathepsin S	2.27	0.026	-0.638
Hs.43857	SULF2	sulfatase 2	0.57	0.01	-0.707
Hs.154078	LBP	lipopolysaccharide binding protein	0.44	0.028	-0.629
Hs.156316	DCN	decorin	0.38	0.024	-0.644
Hs.10844	LRG1	leucine-rich alpha-2-glycoprotein 1	0.18	0.036	0.609
Hs.164226	THBS1	THBS1 thrombospondin 1	0.05	0.003	-0.772
Hs.306051	WNT5B	WNT5B wingless type MMTV integration site family member 5B	0.05	0.01	0.706
Hs.8230	ADAMTS1	ADAMTS1 a disintegrin like and metalloprotease (reprolysin type) with thrombospondin type 1 motif	0.05	0.014	-0.687
Hs.212581	MMP24	MMP24 matrix metalloproteinase 24 (membrane inserted)	0.05	0.03	0.623
Hs.64016	PROS1	PROS1 protein S (alpha)	0.03	0.033	-0.615
Hs.401316	IGFBP1	IGFBP1 insulin like growth factor binding protein 1	0.01	0.009	0.711

MCR, metabolic clearance rate.

Table S3. Clinical Characteristics of the Human Subjects Whose Blood Was Sampled, Related to Figure 1

n	35
Age (years)	58.6±12.0
Sex (M/F)	22/13
Body mass index (kg/m^2)	25.2±4.3
Fasting plasma glucose (mg/dl)	171.0±51.0
HOMA-IR	2.53±1.56
HbA1c (%)	9.1±2.0
Total cholesterol (mg/dl)	196.3±31.7
Triglyceride (mg/dl)	126.8±60.0

Data are mean ± S

HOMA-IR, homeostasis model assessment for insulin resistance; HbA_{1c}, hemoglobin A_{1c}. Blood was sampled following overnight fasting. All subjects had been diagnosed with type 2 diabetes.

Table S4. Clinical Characteristics of Type 2 Diabetes Patients and Control Subjects Whose Blood Was Sampled, Related to Figure 1

	NGT	DM
n	9	12
Age (years)	40.4±14.4	48.3±10.3
Sex (M/F)	3/6	5/7
Height (cm)	161.4±12.3	167.8±6.8
Body weight (kg)	62.8±13.4	75.7±20.0
Fasting plasma glucose (mg/dl)	94.4±7.9	213.1±57.1**
HOMA-IR	1.43±0.57	2.74±1.9+

Data are mean ± SD

** $p<0.01$ vs NGT

+ $p=0.055$ vsNGT

NGT, normal glucose tolerance; HOMA-IR, homeostasis model assessment for insulin resistance. Blood was sampled following overnight fasting.

Table S5. Metabolic Characteristics of KK and KKAy Mice, Related to Figure 1

	KK	KKAy
Body weight (g)	36.0±3.0	39.3±1.4^{+}
Food intake (g/day)	3.7±0.3	4.2±0.4*
Liver weight (g)	1.5±0.4	1.9±0.1*
Liver trigliceride content (mg/g liver)	32.5±16.2	57.3±19.4^{++}
Epididymal fat weight (g)	0.6±0.02	0.8±0.05*
Fasting blood glucose (mg/dl)	132.2±10.3	191.8±20.2**
Fasting insulin	1.1±0.2	3.0±1.5*

Data are mean ± SD

$^{**}p<0.01$ vs KK

$^{*}p<0.05$ vs KK

$^{+}$ $p=0.059$ vs KK

$^{++}$ $p=0.081$ vs KK

Supplemental References

DeFronzo, R. A., Tobin, J. D., and Andres, R. (1979). Glucose clamp technique: a method for quantifying insulin secretion and resistance. Am J Physiol *237*, E214-223.

Kubota, N., Terauchi, Y., Kubota, T., Kumagai, H., Itoh, S., Satoh, H., Yano, W., Ogata, H., Tokuyama, K., Takamoto, I., *et al.* (2006). Pioglitazone ameliorates insulin resistance and diabetes by both adiponectin-dependent and -independent pathways. J Biol Chem *281*, 8748-8755.

Matthews, D. R., Hosker, J. P., Rudenski, A. S., Naylor, B. A., Treacher, D. F., and Turner, R. C. (1985). Homeostasis model assessment: insulin resistance and beta-cell function from fasting plasma glucose and insulin concentrations in man. Diabetologia *28*, 412-419.

Misu, H., Takamura, T., Matsuzawa, N., Shimizu, A., Ota, T., Sakurai, M., Ando, H., Arai, K., Yamashita, T., Honda, M., *et al.* (2007). Genes involved in oxidative phosphorylation are coordinately upregulated with fasting hyperglycaemia in livers of patients with type 2 diabetes. Diabetologia *50*, 268-277.

Nagai, Y., Takamura, T., Nohara, E., Yamashita, H., and Kobayashi, K. (1999). Acute hyperinsulinemia reduces plasma concentrations of homocysteine in healthy men. Diabetes Care *22*, 1004.

Reid, B. N., Ables, G. P., Otlivanchik, O. A., Schoiswohl, G., Zechner, R., Blaner, W. S., Goldberg, I. J., Schwabe, R. F., Chua, S. C., Jr., and Huang, L. S. (2008). Hepatic overexpression of hormone-sensitive lipase and adipose triglyceride lipase promotes fatty acid oxidation, stimulates direct release of free fatty acids, and ameliorates steatosis. J Biol Chem *283*, 13087-13099.

Saito, Y., Watanabe, Y., Saito, E., Honjoh, T., and Takahashi, K. (2001). Production and application of monoclonal antibodies to human selenoprotein P. Journal of Health Science *47*, 346-352.

Sakurai, M., Takamura, T., Ota, T., Ando, H., Akahori, H., Kaji, K., Sasaki, M., Nakanuma, Y., Miura, K., and Kaneko, S. (2007). Liver steatosis, but not fibrosis, is associated with insulin resistance in nonalcoholic fatty liver disease. J Gastroenterol *42*, 312-317.

Watanabe, A., Tsuneishi, E., and Takimoto, Y. (1989). Analysis of ATP and Its Breakdown Products in Beef by Reversed-Phase HPLC. Journal of Food Science *54*, 1169-1172.

Histological Course of Nonalcoholic Fatty Liver Disease in Japanese Patients

Tight glycemic control, rather than weight reduction, ameliorates liver fibrosis

ERIKA HAMAGUCHI, MD, PHD[1]
TOSHINARI TAKAMURA, MD, PHD[1]
MASARU SAKURAI, MD, PHD[2]
EISHIRO MIZUKOSHI, MD, PHD[3]
YOH ZEN, MD, PHD[4]
YUMIE TAKESHITA, MD, PHD[1]
SEIICHIRO KURITA, MD, PHD[1]
KUNIAKI ARAI, MD, PHD[3]
TATSUYA YAMASHITA, MD, PHD[3]
MOTOKO SASAKI, MD, PHD[5]
YASUNI NAKANUMA, MD, PHD[5]
SHUICHI KANEKO, MD, PHD[3]

OBJECTIVE — The goal of this study was to examine whether metabolic abnormalities are responsible for the histological changes observed in Japanese patients with nonalcoholic fatty liver disease (NAFLD) who have undergone serial liver biopsies.

RESEARCH DESIGN AND METHODS — In total, 39 patients had undergone consecutive liver biopsies. Changes in their clinical data were analyzed, and biopsy specimens were scored histologically for stage.

RESULTS — The median follow-up time was 2.4 years (range 1.0–8.5). Liver fibrosis had improved in 12 patients (30.7%), progressed in 11 patients (28.2%), and remained unchanged in 16 patients (41%). In a Cox proportional hazard model, decrease in A1C and use of insulin were associated with improvement of liver fibrosis independent of age, sex, and BMI. However, ΔA1C was more strongly associated with the improvement of liver fibrosis than use of insulin after adjustment for each other (χ^2; 7.97 vs. 4.58, respectively).

CONCLUSIONS — Tight glycemic control may prevent histological progression in Japanese patients with NAFLD.

Diabetes Care 33:284–286, 2010

Accumulating trans-sectional evidence suggests that the presence of multiple metabolic disorders, including obesity, diabetes, dyslipidemia, hypertension, and ultimately metabolic syndrome, are associated with nonalcoholic fatty liver disease (NAFLD) (1). However, it remains unclear which metabolic abnormalities are responsible for the pathological progression of NAFLD, especially in Japanese patients, who generally are not severely obese compared with Western patients.

We retrospectively compared clinical features with the histological changes in the livers of Japanese patients with NAFLD who had undergone serial liver biopsies.

RESEARCH DESIGN AND METHODS

— We recruited 195 patients with clinically suspected NAFLD who had undergone liver biopsies at Kanazawa University Hospital from 1997 through 2008. For details about the study subjects and the exclusion criteria, see supplementary Fig. 1 in the online appendix, available at http://care.diabetesjournals.org/cgi/content/full/dc09-0148/DC1. Of 178 patients diagnosed histologically as having NAFLD, 39 had undergone serial liver biopsies.

Data collection

Clinical information, including age, sex, body measurements, and prevalence of metabolic abnormalities, was obtained for each patient. Venous blood samples drawn for laboratory testing before the liver biopsies were obtained. All subjects had been administered a 75-g oral glucose tolerance test at baseline and at follow-up.

Liver biopsies

Biopsies were obtained after a thorough clinical evaluation and receipt of signed informed consent from each patient. All biopsies were analyzed twice and at separate times randomly by a single pathologist who was blinded to the clinical information and the order in which the biopsies were obtained. The biopsied tissues were scored for steatosis, stage, and grade as described (2), according to the standard criteria for grading and staging of nonalcoholic steatohepatitis proposed by Brunt et al. (3).

For additional details on subjects, data collection methods, liver pathology, and statistical analyses, see supplementary Methods in the online appendix.

RESULTS

— The basal clinical and biochemical data from 39 patients with NAFLD are described in supplementary Table 1. Prevalence of type 2 diabetes, hypertension, and dyslipidemia were 77, 36, and 64%, respectively. The median follow-up period was 2.4 years (range 1.0–8.5). Medications for diabetes and medication changes during the follow-up period are described in supplementary Table 2. Seventeen patients treated with oral diabetic agents were switched to insulin therapy after the initial biopsy. No patients initiated pioglitazone during follow-up.

From the [1]Department of Disease Control and Homeostasis, Kanazawa University Graduate School of Medical Science, Ishikawa, Japan; the [2]Department of Epidemiology and Public Health, Kanazawa Medical University, Ishikawa, Japan; the [3]Department of Gastroenterology, Kanazawa University Hospital, Ishikawa, Japan; the [4]Division of Pathology, Kanazawa University Hospital, Ishikawa, Japan; and the [5]Department of Human Pathology, Kanazawa University Graduate School of Medical Science, Ishikawa, Japan.
Corresponding author: Toshinari Takamura, ttakamura@m-kanazawa.jp.
Received 8 February 2009 and accepted 20 October 2009. Published ahead of print at http://care.diabetesjournals.org on 30 October 2009. DOI: 10.2337/dc09-0148.

Table 1—*Baseline and follow-up clinical features and gradients of laboratory markers associated with changes in liver fibrosis in 39 patients with NAFLD*

	Baseline				Follow-up			
	Improved	Stable	Progressed	*P*	Improved	Stable	Progressed	*P*
n	12	16	11		12	16	11	—
Simple fatty liver:nonalcoholic steatohepatitis (*n*)	3:9	9:7	10:1		10:2	9:7	6:5	
Age (years)	51.5 (29–66)	48.5 (20–79)	51.5 (29–66)	0.97				
Sex (M:F)	5:7	12:4	5:7	0.17				
BMI (kg/m^2)	27.5 (23.2–34.1)	27.7 (22.5–44.4)	30.9 (23.4–37.7)	0.74	26.9 (22.8–31.2)	29.1 (24.3–44.8)	30.7 (24.1–36.3)	0.13
Aspartate transaminase (IU/l)	70 (11–106)	29 (14–86)	32 (13–83)	0.05	23 (11–28)	26 (15–71)	24 (14–164)	0.20
Alanine transaminase (IU/l)	71 (10–209)	48 (23–81)	40 (11–162)	0.13	21 (11–53)	36 (21–66)	31 (12–202)	0.10
Fasting plasma glucose (mg/dl)	133 (96–207)	143 (87–414)	111 (76–167)	0.20	103 (93–220)	121 (83–198)	116 (88–199)	0.51
A1C (%)	8.2 (4.7–11.6)	8.0 (4.9–13.6)	6.2 (5.1–9.5)	0.27	6.0 (5.0–9.0)	6.2 (5.0–10.0)	7.0 (6.0–11.0)	0.10
HOMA-IR	3.9 (0.7–5.5)	3.4 (1.9–7.7)	3.9 (1.6–11.1)	0.91	3.1 (1.5–8.5)	3.4 (1.9–7.7)	3.9 (1.6–11.1)	0.76
QUICKI	0.32 (0.29–0.40)	0.31 (0.27–0.34)	0.31 (0.29–0.35)	0.32	0.33 (0.28–0.37)	0.32 (0.30–0.35)	0.31 (0.29–0.34)	0.82
Muscle insulin resistance	2.1 (1.5–4.0)	1.7 (0.3–3.3)	3.0 (2.1–4.4)	0.20	2.0 (1.3–5.9)	2.4 (1.6–4.5)	1.9 (1.3–4.5)	0.80
Hepatic insulin resistance ($\times 10^6$)	5.3 (2.3–10.2)	5.0 (2.3–10.0)	3.7 (1.4–10.6)	0.66	3.9 (1.4–9.8)	4.3 (1.9–15.9)	4.5 (2.3–8.8)	0.75
Total cholesterol (mg/dl)	191 (128–276)	187 (129–252)	206 (163–244)	0.57	192 (114–224)	195 (136–273)	194 (162–234)	0.74
Triglycerides (mg/dl)	111 (28–224)	114 (36–204)	96 (36–521)	0.87	104 (22–241)	115 (57–241)	131 (36–173)	0.68
HDL cholesterol (mg/dl)	47 (35–82)	51 (31–73)	48 (20–74)	0.68	53 (40–71)	52 (39–64)	52 (36–79)	0.92
Platelets ($\times 10^4/\mu$l)	21.1 (9.4–30.8)	23.0 (7.0–38.2)	24.3 (20.2–41.2)	0.29	23.3 (14.5–27.6)	21.5 (6.3–31.8)	24.0 (15.2–32.6)	0.60
Ferritin (μg/dl)	185 (13–452)	397 (190–604)	46 (10–347)	0.14	74 (16–211)	162 (110–614)	62 (10–171)	0.05
hs-CRP	0.40 (0.08–7.53)	0.14 (0.02–0.61)	0.06 (0.00–0.30)	0.23	0.09 (0.04–0.23)	0.10 (0.00–0.24)	0.09 (0.00–0.89)	0.89
Type IV collagen 7S (ng/dl)	5.1 (2.7–10.0)	4.1 (3.1–7.2)	3.7 (3.3–4.5)	0.27	3.5 (2.3–3.9)	8.3 (3.2–14.0)	4.0 (3.2–5.0)	0.21
HA (ng/dl)	20.6 (0.0–144.7)	25.5 (11.5–299)	30.4 (0.0–61.7)	0.66	32.8 (0.0–117.2)	24.5 (0.0–570)	24.3 (0.0–140.3)	0.63
P-III-P (U/ml)	0.6 (0.5–1.2)	0.6 (0.4–45.0)	0.5 (0.4–0.6)	0.07	0.6 (0.3–0.8)	0.5 (0.5–233.0)	0.6 (0.4–1.0)	0.96
Diabetes (%)	82	69	64	0.59	82	75	64	0.56
Dyslipidemia (%)	73	63	73	0.95	73	63	73	0.86
Hypertension (%)	64	18	36	0.03	64	18	36	0.10
Metabolic syndrome (%)	73	38	27	0.18	67	50	45	0.43
ΔA1C					−1.9 (−6.0 to 0.4)	−1.2 (−6.1 to 4.4)	0.3 (−1.8 to 7.1)	0.02
ΔBody weight					−4.7 (−10.6 to 10.2)	2.2 (−9.4 to 13.4)	−0.9 (−12.7 to 9.6)	0.04
ΔHOMA-IR					−1.3 (−4.4 to 1.2)	−0.3 (−4.3 to 3.3)	−0.7 (−6.1 to 1.8)	0.81

Data are medians (range) or %. A Kruskal-Wallis test and a χ^2 test were used to compare the continuous and categorical variables among three groups. HA, hyaluronic acid; hs-CRP, high-sensitivity C-reactive protein; P-III-P, procollagen III peptide.